ACS ES&T Water

Open Access

pubs.acs.org/estwater

Article

Fluorescence-Based Indicators of *Escherichia coli* and Untreated Wastewater: Turbidity Correction and Comparison of *In Situ* and Benchtop Fluorometers in a Sewage-Polluted Urban River

Trent Biggs,* Natalie Mladenov, Stephany Garcia, Yongping Yuan, Daniel Sousa, Alexandra Grant, Elise Piazza, Trinity Magdalena-Weary, Callie Summerlin, and Doug Liden

Cite This: *ACS EST Water* 2025, 5, 2212−2222

Read Online

ACCESS | Metrics & More | Article Recommendations | Supporting Information

ABSTRACT: Fluorescence-based sensors of tryptophan (TRP) and chromophoric dissolved organic matter (CDOM) can provide real-time information on water quality. We 1) evaluate the accuracy of benchtop (Aqualog) and *in situ* (Manta) fluorometers for estimating percent untreated wastewater (pctWW) in laboratory experiments; 2) propose a correction for turbidity; 3) test for correlations between TRP or CDOM and *Escherichia coli* (*E. coli*) concentrations in river water samples; and 4) quantify the impact of stormflow on wastewater discharge and bacteria in the Tijuana River. In laboratory experiments, Aqualog TRP correlated closely with pctWW ($R^2 > 0.98$), while Manta TRP increased with pctWW up to 20−50% but then decreased thereafter. In river water samples, Aqualog TRP and CDOM had stronger correlations with *E. coli* concentrations than did Manta TRP, which correlates with *E. coli* but the relationship varies by event. Wastewater flow ($m^3\ s^{-1}$) increased during storm events, but much less than total storm discharge, so the percent wastewater decreased during storms. Benchtop fluorometers provide reliable estimates of wastewater percentage and bacteria concentrations, while *in situ* fluorometers indicate wastewater and bacteria presence, but may not provide reliable estimates in highly polluted waters or stormflow without further correction of turbidity, inner filter effects, and variations among storm events.

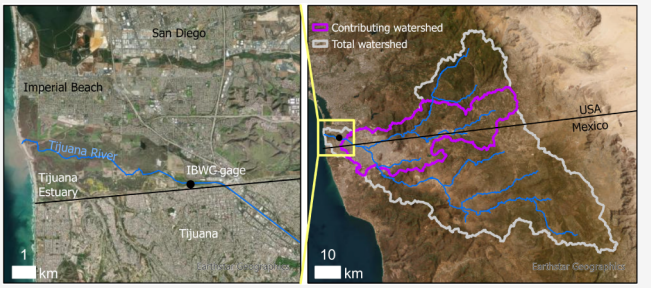

KEYWORDS: *dissolved organic matter, sewage, interference, pathogens, real-time monitoring*

1. INTRODUCTION

Wastewater and pathogenic bacteria are common contaminants in surface water but are expensive and difficult to monitor at high spatial and temporal resolution. Real-time monitoring of wastewater contamination, fecal indicator bacteria (FIB) and other associated contaminants is critical for rapid management action to mitigate human contact with polluted water. Data on water quality with high temporal resolution is also needed for accurate determination of concentration-discharge and load-discharge relationships, which can help identify sources and suggest management actions, but collection of grab-samples at sufficient temporal resolution can be cost prohibitive and time-consuming. Storm events are particularly important for contaminant loading to receiving waters[1,2] and information on the concentration and load of contaminants during baseflow and stormflow is essential for understanding contamination of receiving waters and for establishing boundary conditions for models of ocean water quality,[3] but storms are difficult and costly to sample.

Fluorescence-based sensors (fluorometers) can provide proxy measurements for wastewater and FIB concentrations, both in the laboratory and with *in situ* sensors.[4−10] Tryptophan-like fluorescence (TRP) and chromophoric dissolved organic matter (CDOM) in particular can indicate wastewater contamination and FIB.[8,11−15] Portable *in situ* sensors have been developed for measurement of TRP and CDOM in streams, which can supplement water sampling and can be integrated into telemetry for near real-time monitoring of water quality. Real-time information on TRP and CDOM at high temporal resolution can provide insights into the behavior of wastewater and bacteria during storm and nonstorm events, helping to identify sources and determining concentration-discharge and load-discharge relationships.

Several interferences complicate measurement of TRP and CDOM in surface waters, including turbidity,[12] temperature,[16] and inner filter effects,[17−19] where organic compounds absorb light that is emitted from the sensor and from the compound

Received: November 9, 2024
Revised: April 15, 2025
Accepted: April 17, 2025
Published: April 29, 2025

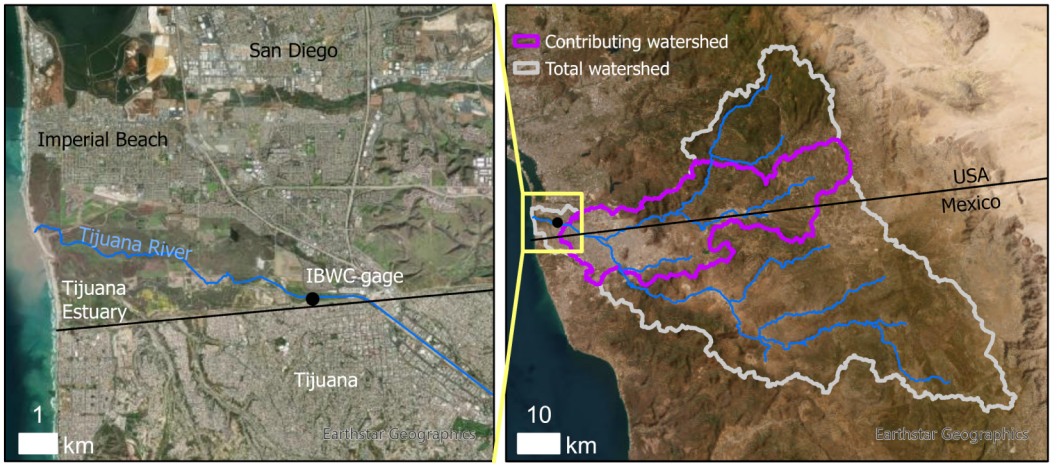

Figure 1. Sampling location at the IBWC stream gage (left) and location in the Tijuana River Watershed (right).

of interest (TRP or CDOM). Fluorescence spectra acquired with benchtop fluorometers can be corrected for inner-filter effects,[20] but such corrections cannot be performed by existing *in situ* sensors that typically have one excitation−emission pair. Turbidity is often high (>500 FNU) during storm events, but field-testing of TRP sensors in streamwater is rare, particularly during storms with highly variable turbidity (but see.[8] Turbidity of 1000 FNU depresses fluorescence readings by up to 70% (TRP[12]) and 90% (CDOM[21]) though impacts differ by particle size.[12] Khamis et al. (2015) documented an increase in TRP fluorescence for turbidity less than 100 NTU of clay particles, with decreases in TRP at turbidity higher than 100 NTU, and so proposed a third-order polynomial as a correction factor. Downing et al. (2012) showed monotonic decreases in CDOM fluorescence with increasing turbidity, with Beer−Lambert-like attenuation. Water samples for benchtop fluorometers are filtered prior to analysis, removing interference from turbidity, but such samples are labor-intensive to obtain and require time to analyze, incentivizing the development of turbidity correction functions for *in situ* TRP and CDOM sensors. Turbidity interference is a major complication when using TRP and CDOM to estimate bacteria concentrations in surface waters, restricting many applications to groundwater[9] or drinking water.[15]

In this study, we compare fluorescence values (TRP and CDOM) recorded by portable, submersible *in situ* sensors (Manta) with fluorescence recorded by a benchtop fluorometer (Aqualog) and with *Escherichia coli* (*E. coli*) concentrations in both laboratory experiments and in water samples collected from a contaminated urban stream, the transboundary Tijuana River, during both baseflow (dominated by untreated wastewater) and stormflow. Laboratory experiments included adding wastewater to stream and ocean water and quantifying the TRP and CDOM response. The *in situ* sensor was installed to continuously measure TRP, CDOM, and turbidity in the river. Water samples were collected from the river during stormflow and baseflow conditions, and the samples analyzed for Aqualog TRP, CDOM and bacteria concentrations for comparison with the Manta readings. Our objectives are to determine the relationship between wastewater percentage and fluorescence in the laboratory, to develop and apply turbidity corrections to streamwater samples collected under stormflow and dry weather conditions, and to use the results to better understand the relationship between discharge, fluorescence, wastewater percentage, and *E. coli* concentrations and loads in an urban river with persistent untreated wastewater flow.

2. STUDY AREA

The Tijuana River watershed drains 4483 km^2, 27% of which is in the United States and 73% in Mexico (Figure 1).[22] Dams impound 71% of the drainage area, so the actively contributing drainage area is 1138 km^2 and includes most of Tijuana (population 1.9 million in 2020) and all of Tecate (population 0.1 million in 2020.[23] The watershed has 36,900 cattle, 5000 pigs and an estimated 400,000 to 750,000 poultry[24] (see SI1, Table S1). The climate is Mediterranean: mean annual rainfall in the contributing drainage area was 327 mm and mean annual runoff was 35 mm (32 MCM) in water years 2001−2020,[22] with most rainfall and runoff occurring between November and March. Mean annual temperature ranges from 13 to 19 °C, and mean monthly temperature is 7 to 14 °C higher in July compared to December (years 1972−1989.[25]) The geology of the contributing drainage area is Peninsular Range granites in the east and marine and fluvial sediments in the west.[26]

Some of the wastewater generated in Tijuana is treated in wastewater treatment plants (WWTPs) in Mexico (Arturo Herrera and La Morita), and the treated wastewater is discharged into the Tijuana River (Figure S1). Downstream of the WWTPs, additional untreated wastewater enters the Tijuana River.[27] A system of pumps diverts some of the river discharge to the International Treatment Plant in the United States (PITAR in Figure S1) and the remainder is diverted to the coast,[27] but the system has been periodically out of service, with nearly continuous nonoperation starting in January 2022. The resulting increase in untreated wastewater discharge entering the ocean has resulted in continuous beach closures due to elevated FIB concentrations.[28,29]

3. METHODS AND PROCEDURE

The methods consist of a) Method Development, including wastewater addition experiments (Section 3.1) and turbidity correction (3.2) and b) Method Application to river samples collected in the Tijuana River (3.3 and 3.4). All methods compared submersible sensors (Manta) with a benchtop fluorometer (Aqualog). Briefly, the Method Development sections determined the relationship between percent waste-

https://doi.org/10.1021/acsestwater.4c01092
ACS EST Water 2025, 5, 2212−2222

water and fluorescence in laboratory experiments (3.1), and proposed an equation to correct for the impact of turbidity on fluorescence of the submersible sensors (3.2). The Method Application sections tested for the correlation between fluorescence and *E. coli* concentrations in river water samples, with and without turbidity correction (3.3), estimated the percent wastewater during storms and dry weather, and analyzed the relationship between river discharge and major water quality constituents, including *E. coli*, fluorescence, turbidity, and estimated wastewater discharge (3.4).

3.1. Method Development: Wastewater Addition Experiments. Wastewater addition experiments were conducted in the laboratory on three separate dates (SI2, Table S2). Untreated wastewater was obtained from the inlet to the International Wastewater Treatment Plant in San Diego. In two of the three experiments, the wastewater was added to seawater (Seawater1, Seawater2), and in the third experiment wastewater was added to streamwater (Streamwater) collected from Alvarado Creek in San Diego, which is less polluted than the Tijuana River[8] (Table S2). Seawater was chosen for two experiments, as the original goals of the addition experiments included determining the percent wastewater in the Tijuana Estuary to complement ongoing monitoring there,[28] and because seawater had lower background values of CDOM than the streamwater at Alvarado Creek.

Wastewater was added to ocean or streamwater to create a mixture with percentages of wastewater ranging from 10 to 90%. TRP, CDOM and turbidity of the water-wastewater mixtures was measured continuously with a Manta sonde.[30] The CDOM sensor is Turner Designs 2300-251 (SN 12215259; excitation 470, emission 60 nm), and the tryptophan sensor is Turner Designs 2300-256 (SN 12215259; excitation 350, emission 55 nm in the UV range). The turbidimeter measures scattering of near-infrared light (700−1000 nm) at 90 deg to an introduced beam of infrared light (Turner Designs SN 1901), and is an ISO 7027 sensor type (±2% of reading, 0−1000 FNU, ± 4% of reading, 1000−4000 FNU). Three different Manta sondes were used during the experiments; calibration logs for TRP show that they had very similar calibration curves and so their results can be directly compared (Figure S2, Table S3).

Water samples were collected from each 10% increment of the wastewater-seawater or wastewater-streamwater mixture and from the undiluted wastewater. The samples were filtered through 0.7 μm glass fiber filters precombusted at 500 °C for 2 h. Fluorescence and UV and visible light absorbance were measured on a Horiba Aqualog Fluorometer using a quartz cuvette, path length 1 cm, integration time 0.25 s. Raw values were corrected for inner filter effects in Matlab using the absorbance correction specified in ref 17. Additional corrections included blank subtraction, Raman normalization at 350 nm to provide intensities in Raman Units (RU), and Rayleigh scatter masking.[8] Fluorescence intensities (RU) were acquired at TRP and CDOM wavelengths corresponding to those recorded by the *in situ* Manta TRP sensor (ex 285 nm/em 350 nm) and Manta CDOM sensor (ex 325 nm/em 470 nm). TRP standards of 100 ppb were prepared from dry tryptophan powder (CAS 73-22-3, Fisher Scientific bioreagents) and CDOM standards of quinine sulfate (300 ppb) were prepared in 0.1 N sulfuric acid. Linear regression models were developed for predicting pctWW as a function of TRP and CDOM from both instruments (Aqualog and Manta). Separate regressions were created for each experiment.

3.2. Method Development: Turbidity Correction Factor. We propose an exponential turbidity correction function for TRP measured by the submersible sensor (Manta):

$$TRP_{TC} = TRP_{raw} e^{kTURB} \quad (1)$$

where TRP_{TC} is TRP corrected for turbidity, TRP_{raw} is the value measured by the sensor, k is a coefficient, and TURB is turbidity in FNU. Aqualog TRP does not need turbidity correction because samples are filtered in the laboratory prior to analysis. eq 1 differs from Khamis et al. (2015), who use a third-order polynomial, which results in unrealistic values outside the calibration range. eq 1 is consistent with a Beer−Lambert Law-type correction for light attenuation through a translucent substance, and is similar to a turbidity correction developed for CDOM.[21] A TRP depression factor due to turbidity can then be calculated as $TRP_{raw}/TRP_{TC} = e^{-kTURB}$. Based on results from turbidity augmentation experiments in the laboratory (Section SI4), we also tested a power function for the turbidity correction factor (eq S1), but used the exponential function (eq 1) for the correction of *in situ* measurements. The parameters in the turbidity correction eq 1 were determined by calibrating k to field measurements of turbidity and *E. coli* (Section 3.3.1) and compared with the laboratory experiments and other literature (Section SI4, Figure S3). The R^2 and root-mean-square error (RMSE) of the relationship between *E. coli* and TRP or CDOM were compared for a range of k values, and the k value with the highest R^2 selected for the final turbidity correction.

3.3. Method Application: Stream Water Monitoring. *3.3.1. In situ Measurements.* The Manta sonde (Section 3.1) was deployed in the Tijuana River approximately 10 m upstream of a stream gauge and weir maintained by the International Boundary and Water Commission (IBWC, 32.5433° N, 117.0503° W, Figure 1). The sonde was housed in a 4" diameter PVC pipe, and sensors were approximately 15 cm off the channel bed. The Manta collected readings at 10 min intervals and the data transmitted in near-real time to a Web site and archiving service, wqdatalive. The channel bed was dry at the time of installation (Nov 3, 2022) and consisted of large gravel and small boulders, with no fine sediment accumulation. Discharge in the river began and the sonde started recording data on Nov 8, 2022. The sonde remained submerged for the rest of the sampling period except for 1 week (Dec 3−11) when conductivity was near zero (See SI5 and Figure S4 for the discharge time series for the monitored period). Optical fluorescence and turbidity sensors are not impacted by periods of nonsubmergence, are typically stored dry,[30] and the stability of subsequent calibrations and standards checks confirm that the sensors were not impacted by the short dry periods. Sedimentation in the housing of the sensor occurred periodically and was cleaned following storm events.

All sensors on the Manta were calibrated prior to deployment, and either recalibrated or checked against known standards (100 ppb TRP, 300 ppb CDOM) at one- to three-month intervals. The TRP and CDOM sensors were also checked against solid standards. The turbidity sensor was checked against either 100 or 1000 FNU AMCO clear turbidity standards for ISO 7027 probes. The CDOM sensor was checked against solid standards near the beginning (Jan 2023) and after the end (Jul 2023) of the deployment period, and against a quinine sulfate standard near the beginning of the

https://doi.org/10.1021/acsestwater.4c01092
ACS EST Water 2025, 5, 2212−2222

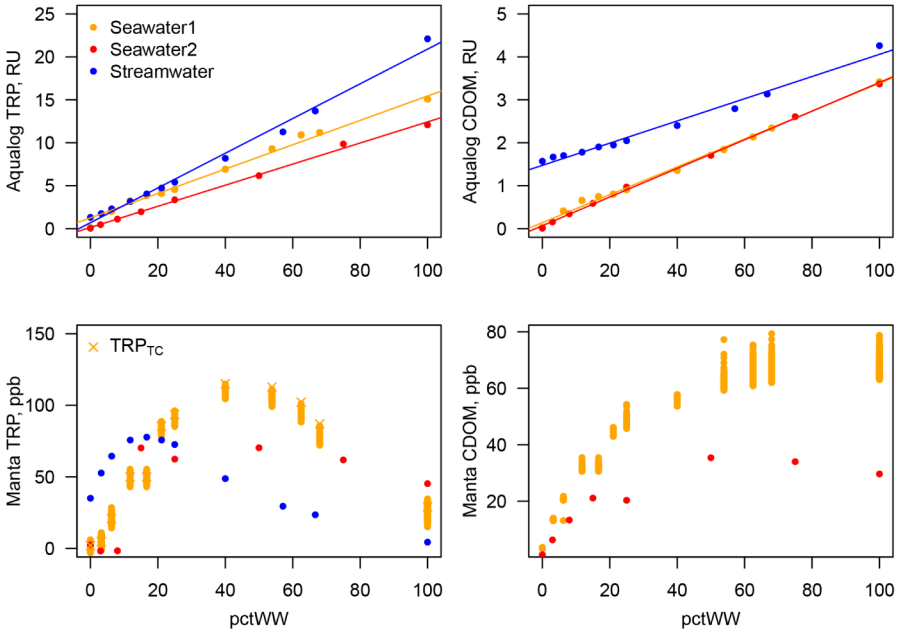

Figure 2. Percent wastewater versus fluorescence of TRP (left) and CDOM (right) from Aqualog (top) and Manta (bottom) for three wastewater addition experiments (Table S2). Manta TRP and CDOM are without turbidity correction due to low turbidity. TRP_{TC} is TRP corrected for turbidity using eq 1 and was performed only for Seawater1 due to the small impact of turbidity correction.

deployment (11/30/2022); all readings of CDOM on both solid and liquid standards differed by less than 10%, so CDOM was not adjusted further. TRP showed signs of downward drift in raw value (RV, mV) for the 100 ppb TRP standard during the first few months of deployment, after which RV readings for the 100 ppb standard stabilized (Figure S2). For TRP, the calibration errors were sometimes high (>20%), so we also recalculated the raw value (RV in mV) from the sensor using the coefficients in the calibration log, and recalculated TRP and turbidity with a standard calibration curve determined from the average of the previous calibrations. The turbidimeter showed consistency in the relationship between standard concentration and RV, so no recalibration was necessary. See Supporting Information for details on the calibration and standards checks (Figures S2 and S5, Table S3).

Temperature correction factors were applied to TRP and CDOM.[16] The correction varies with the concentration of TRP and CDOM; here, a temperature coefficient of fluorescence value (ρ in ref 16) of −0.01 was used. The temperature correction was relatively small, changing TRP and CDOM by less than 10% for all samples. Water temperature was also similar among sampled events, resulting in similar mean correction factors (0.94 for 2022−12 and 2023−02 events; 1.0 for 2023−05).

3.3.2. Stream Water Sampling and Laboratory Analysis. Water samples were collected hourly over four 24-h events using a Teledyne ISCO 6712 autosampler. Bottles were rinsed in bleach and autoclaved prior to deployment. The four events included three storm events (December 2022, two in February 2023) and one nonstorm event (May 2023) when streamflow was dominated by wastewater.

E. coli concentrations were quantified in the unfiltered water samples within 24 h of collection. The U.S. EPA[31] recommends that the time from sample collection to placement of the sample in the incubator for total coliforms and fecal coliforms in surface water sources must not exceed 8 h, but samples collected by the autosampler at the beginning of the sampling period could not be retrieved in under 8 h due to hazardous conditions in the floodplain. Ice was placed into the autosampler's internal chamber at the start of each autosampler deployment to maintain low temperatures and inhibit biological activity. During methods development, we tested the effect of holding times on four field samples: *E. coli* concentrations differed by less than 10% when analyzed 6 and 30 h after collection (unpublished data). The *E. coli* concentrations in field samples also spanned several orders of magnitude so any changes from holding times will likely be small compared to the overall variability.

E. coli counts per 100 mL were quantified using IDEXX Colilert-18 for samples that underwent serial dilution. Quanti-trays with the sample and reagent were incubated at 35 ± 0.5 °C for 18 h. The counts of positive wells in the Quanti-trays were converted to concentrations of most probable number (MPN) per 100 mL with the IDEXX MPN calculator. Results of dilutions in which counts exceeded the maximum capacity of the IDEXX tray (i.e., all wells were positive) were excluded from the analysis. Field blanks, which are considered sterility controls (EPA, 2005), were employed for every storm sampling event and consistently showed no positive wells for total coliforms or *E. coli*. Samples were filtered through 0.7 μm pore size glass fiber filters and fluorescence spectra were acquired on the filtered samples using the benchtop Horiba Aqualog fluorometer (Section 3.1).[28] TRP, CDOM, temperature, and turbidity values were recorded by the Manta that was deployed in the river during the events. The Manta turbidimeter failed during the May 2023 event due to fouling, so we measured TRP, CDOM, and turbidity for the May 2023 event in the laboratory using the Manta on the samples collected by the autosampler, within 24 h of collection.

3.4. Storm Load Calculations and Wastewater Estimation. Instantaneous untreated wastewater load (m^3 s^{-1}) in the Tijuana River was calculated for each river sample as the product of the pctWW-TRP relationship from the wastewater addition experiments (Section 3.1) and the water

https://doi.org/10.1021/acsestwater.4c01092
ACS EST Water 2025, 5, 2212−2222

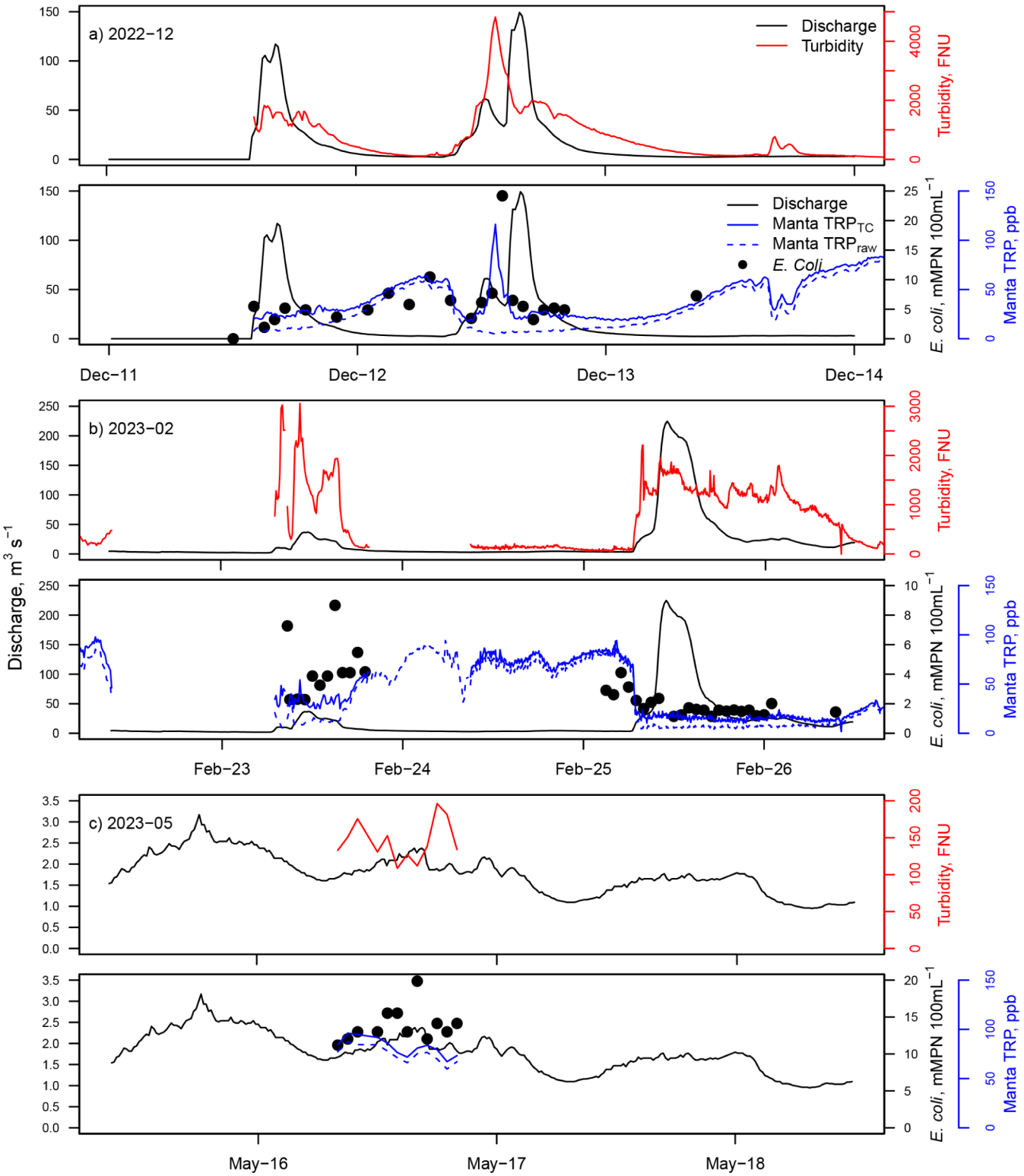

Figure 3. Time series of river discharge, turbidity, Manta TRP (TRP *raw*), Manta TRP corrected for turbidity (Manta TRP_{TC}), and *E. coli* for the a) December 2022 event, b) two February 2023 events and c) May 2023 event. mMPN is million Most Probable Number.

discharge at the time of collection as recorded at the IBWC gage. The best sensor (Aqualog or Manta) and constituent (TRP or CDOM) for predicting pctWW was selected based on the results of the wastewater addition experiments that had: 1) low readings for zero percent wastewater, 2) monotonic, linear relationship with percent wastewater and 3) high R^2 of the prediction of percent wastewater in a linear regression model.

3.5. Statistical Analysis. Univariate regression models were created for predicting *E. coli* from TRP or CDOM in the river water samples. Regressions were performed on both untransformed and log-transformed variables; both *E. coli* and TRP or CDOM were log-transformed for the log-regressions. Additional regressions were performed including the event date as a dummy variable. Aqualog TRP and CDOM were

https://doi.org/10.1021/acsestwater.4c01092
ACS EST Water 2025, 5, 2212−2222

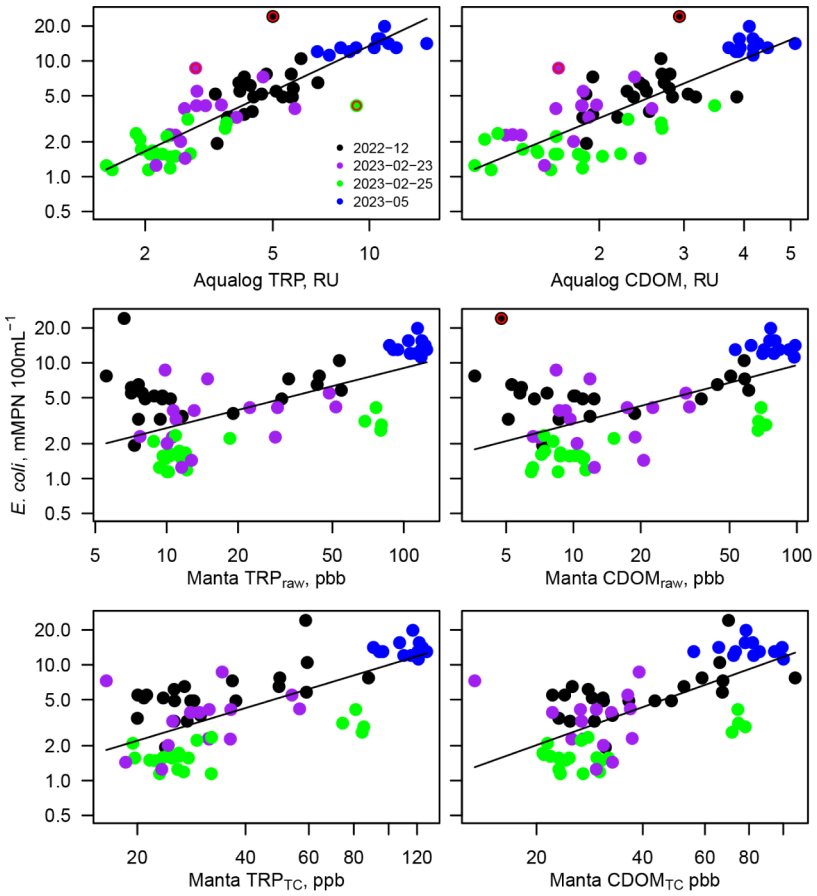

Figure 4. *E. coli* concentrations versus TRP (left panels) and CDOM (right panels), on logarithmic axes, for the benchtop Aqualog (top), *in situ* fluorometer (Manta) without turbidity correction (middle) and Manta with turbidity correction (bottom), k = 0.00065 for TRP, k = 0.0008 for CDOM). The red circles indicate Tukey outliers.

measured on filtered samples and so did not require turbidity correction. For Manta TRP and CDOM, the turbidity correction factor (k; eq 1) was varied from −0.0005 to −0.0015 in increments of 0.0001 and the R^2 calculated for each value of k. All regressions were carried out using both all points, and after excluding Tukey outliers, which were identified as points whose residual from the regression was outside of a given Tukey-k value (1.5) times the interquartile range of the regression errors.[32]

4. RESULTS AND DISCUSSION

4.1. Wastewater Addition. The percent wastewater (pctWW) correlated very closely with Aqualog TRP and CDOM in the wastewater addition experiments (Figure 2); R^2 ranged from 0.98 to 1.00 (Table S2). Aqualog TRP was consistently close to zero for zero pctWW, while CDOM was high in the streamwater prior to any wastewater addition, complicating detection of wastewater when using Aqualog CDOM. The differences in the regressions by experiment are due to differences in the TRP or CDOM of 1) the 100 pctWW and 2) initial (0 pctWW) seawater or streamwater used for the experiments. Aqualog TRP of 100 pctWW was 22.1 RU in for the Streamwater experiment but 15.1 for Seawater1 and 12.1 for Seawater2, reflecting differences in TRP of WW collected at the WWTP. The chemical quality of untreated wastewater varies diurnally and seasonally,[33,34] so differences in TRP among different wastewater samples used in our experiments is expected. For each experiment, the points between 0 and 100 pctWW fall along a straight line; since the undiluted wastewater did not have seawater added, the linearity of the TRP- and CDOM-pctWW relationships suggests that the salinity of the water did not have a significant effect, and that, if the TRP or CDOM values in 0 and 100 pctWW are known, pctWW can be calculated for water of any salinity.

The variability in Aqualog TRP and CDOM values for 100 pctWW, while expected, introduces uncertainty in estimates pctWW from TRP in river water if the TRP of 100 pctWW is not known for the date of sampling. Since we did not know the TRP of untreated WW on our river sampling dates, we estimated three values of pctWW in the water samples from the Tijuana River (Section 4.4), using each of the three regression models that use Aqualog TRP and CDOM as predictors (Seawater1, Seawater2, and Streamwater; Figure 2). Ideally, the pctWW in the stream would be estimated from the TRP and CDOM observed in untreated wastewater on the same day as the stream sampling; such samples were not available at the time of sampling. Alternatively, diurnal and seasonal variability in TRP and CDOM of untreated wastewater could be modeled using Julian date, time of day, and hydrologic conditions.

Manta TRP and CDOM correlated positively and linearly with pctWW up to 20−50% depending on the experiment, but decreased with increasing pctWW thereafter (Figure 2). MantaTRP was high in the 0 pctWW sample for the Seawater1 experiment (40 ppb) and for the 100 pctWW sample in the Streamwater (112 ppb); in order to compare among

https://doi.org/10.1021/acsestwater.4c01092
ACS EST Water 2025, 5, 2212−2222

experiments, we subtracted out these baseline values. Manta CDOM values decreased with increasing pctWW for the Streamwater experiment due to experimental error and were left off of Figure 2. Several nonlinear models to predict pctWW from TRP and CDOM, including polygon and power functions, failed for pctWW greater than 50%. Future work could use machine learning to predict pctWW from Manta TRP and CDOM, though we suspect such models would depend on empirically determined interferences of organic matter and turbidity, which could vary by sensor and water type.

4.2. Event Analysis: Chemographs and Turbidity Effects. The turbidity and TRP of Tijuana River water varied widely among sampled events (0 to 125 ppb TRP; turbidity up to 5000 FNU; Figure 3). TRP generally decreased while turbidity increased with increasing discharge. *E. coli* concentrations (million Most Probable Number, hereafter mMPN) were generally highest at low discharges when wastewater was predominant, though some high *E. coli* values were observed on the rising limb of storm hydrographs (Figure 3a).

The relationship between TURB and the TRP depression factor measured in the laboratory varied by sample (Figure S4). We conclude that our turbidity depression values from eq 1 calibrated to field data are similar to and modestly lower than those reported by ref 12 or recorded by agitating field samples. Further work is required to relate the TRP depression factor to sediment characteristics.

4.3. Aqualog Vs Manta TRP and CDOM, and *E. coli* Regression Models. TRP correlated closely with CDOM for a given sensor (Aqualog or Manta) (Figure S6), suggesting that the two measurements were consistent with each other among all events. TRP and CDOM measured in the field by the Manta had only weak correlations with TRP and CDOM measured in the lab by the Aqualog (Figure S7). Similar to the wastewater addition experiments, Manta TRP decreased with increasing Aqualog TRP for high values of Aqualog TRP. The turbidity correction only slightly improved the weak correlation between TRP or CDOM from Aqualog and Manta.

TRP correlated with *E. coli* when all events are analyzed together, but less well for individual events, both in nonlog (Figure S8) and log space (Figure 4). R^2 values were highest for Aqualog TRP (R^2 0.85 without Tukey outlier, log-transformed; Table 1, Table S4) followed by Aqualog CDOM (R^2 0.68). For Manta TRP and CDOM, turbidity correction slightly improved the prediction of *E. coli*. *k* values between 0.0006 and 0.0008 had the highest R^2 (Figure S9). Event date was a significant predictor in all Manta TRP and CDOM models, suggesting that the TRP-*E. coli* and CDOM-*E. coli* relationships varied by event.

4.4. Wastewater Time Series and Concentration-Discharge Relationships. pctWW and wastewater discharge estimated from Aqualog TRP and the linear models from the wastewater addition experiments varied over a much narrower range than discharge (Figures 5 and 6). The mean event discharge varied by a factor of 26, from 2 $m^3\ s^{-1}$ (May 2023) to 53 $m^3\ s^{-1}$ for the largest storm (Figure S10), while the event-mean wastewater discharge varied by a factor of 5, from 0.9 to 1.6 $m^3\ s^{-1}$ for the dry weather event to 2.6−8.0 $m^3\ s^{-1}$ for the storm events. Event-mean pctWW decreased with increasing event-mean discharge, from 45 to 79% for the low-flow event to 7−15% for the largest event (Figure S10). Daily WW discharge calculated from the Aqualog TRP values from two wastewater experiments gave similar results, with a maximum of 120 MGD (Figure S10).

Conductivity, turbidity, pctWW and TRP_{TC} all had strong and consistent relationships with discharge (Figure 6). Conductivity, TRP_{TC}, and *E. coli* decreased with increasing stream discharge, but most samples were above the line representing dilution of constant wastewater discharge (1 $m^3\ s^{-1}$) by rainfall, suggesting that additional sources of contamination were mobilized during storms, such as pit latrines, outhouses, and cesspools, but potentially also livestock feedlots, which can produce high TRP fluorescence (Baker, 2002). Both pctWW and *E. coli* concentrations for a given

Table 1. Regression Statistics for Models Predicting *E. coli* in River Water from TRP or CDOM from Benchtop (Aqualog) and *In Situ* (Manta) Fluorometers, Log-Transformed Variables[a]

		RMSE		R^2_{adj}		
	N.out	All	No out	All	No out	+Event
Benchtop (Aqualog)						
TRP	3	0.40	0.31	0.76	0.85	0.80
CDOM	2	0.49	0.44	0.63	0.68	0.77
In situ (Manta)						
TRP_{raw}	1	0.67	0.60	0.35	0.43	0.76
$CDOM_{raw}$	1	0.68	0.62	0.31	0.39	0.75
TRP_{TC}	0	0.57	0.57	0.50	0.50	0.81
$CDOM_{TC}$	0	0.59	0.59	0.47	0.47	0.77

[a]N.out is the number of Tukey outliers.'All' indicates all data points, and'No out' excludes Tukey outliers. For turbidity correction k = 0.00065 for TRP, k = 0.0008 for CDOM. + Event indicates a regression model with the event date as a dummy variable.

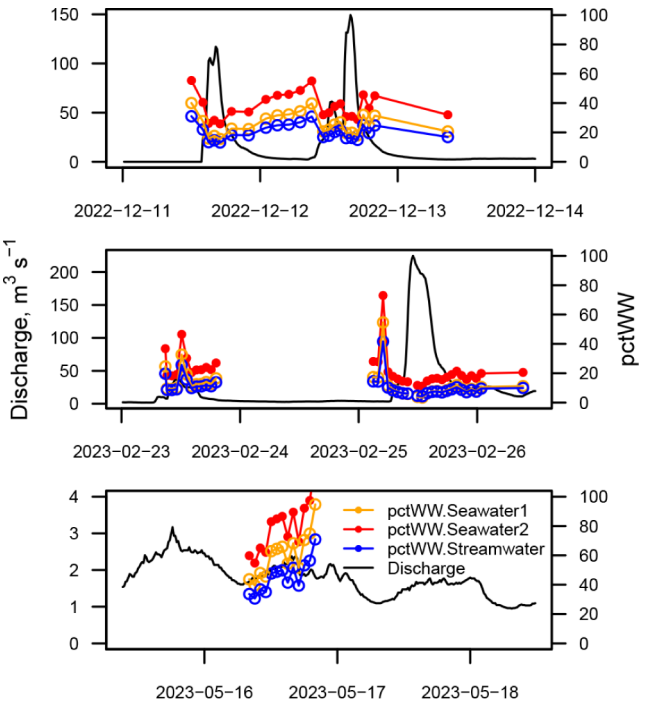

Figure 5. Time series of discharge and percent wastewater (pctWW) for each sampled event, predicted using the observed Aqualog TRP values in the Tijuana river water as input to the pctWW-TRP regression calibrated to the wastewater addition experiments. Three predictions of pctWW are included, one for each WW addition experiment (Figure 2).

https://doi.org/10.1021/acsestwater.4c01092
ACS EST Water 2025, 5, 2212−2222

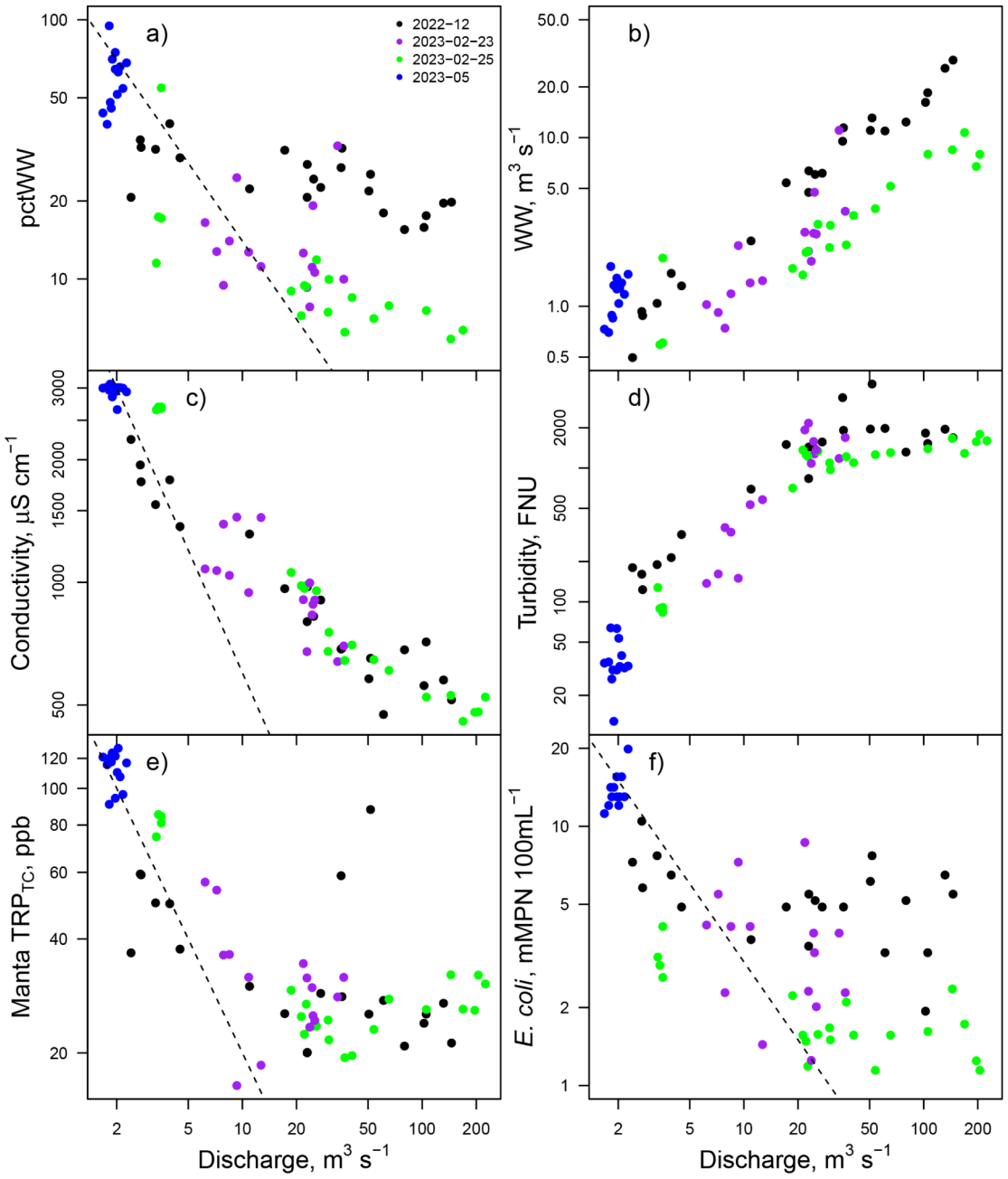

Figure 6. Relationships between instantaneous river water discharge and a) percent wastewater (pctWW) b) wastewater discharge (WW), c) conductivity, d) turbidity, e) TRP corrected for turbidity (TRP_{TC}), and f) *E. coli*, colored by event. The dashed lines indicate dilution of streamflow that is 100% wastewater with a flow rate of 1 $m^3\ s^{-1}$.

water discharge were higher for the 2022−12 event compared to the 2023−02 events (Figure 6). This may be due to differences in the percentage of wastewater that was treated before entering the river, since wastewater treatment reduces TRP values (Mladenov et al., 2018), or to the mobilization and discharge of additional untreated wastewater during events early in the season. Turbidity was also higher during the December event, which is typical of the early wet season when sediment that builds up on hillslopes and in stream channels is transported in overland flow and streamflow. High concentrations of contaminants during storms at the beginning of the wet season is consistent with a "first-flush" mechanism consistently observed in urban streams.[35]

4.5. Wastewater Discharge During Storm Events: Potential Sources. The total flow of untreated wastewater in the Tijuana River estimated from Aqualog TRP (120 million gallons day^{-1}) is larger than the total daily wastewater generation of the portion of Tijuana in the Tijuana River watershed (~80 million gallons day^{-1}), so either wastewater accumulates in the subsurface by sewer exfiltration or in surface stores and is released when there is greater hydrologic connectivity during storm events, some other nonhuman source contributes to TRP and bacteria. A preliminary calculation suggests that daily fecal coliform production from humans in the watershed is 3× larger than from cattle, and much larger than from chickens (38×) and pigs (73×) (Table S1). Our estimated pctWW may include other sources,

https://doi.org/10.1021/acsestwater.4c01092
ACS EST Water 2025, 5, 2212−2222

especially from cattle, but additional work is needed to determine the concentration of TRP and *E. coli* from various nonhuman sources under storm and dry weather conditions. Regardless of the source (human or animal agriculture), Aqualog TRP provides a good proxy for *E. coli*, and pctWW can be interpreted as untreated wastewater from both human and livestock sources, especially during storm events when excreta may be mobilized from pastures and feedlots.

5. CONCLUSION

5.1. In Situ Sensors: Turbidity and Inner Filter Effects. Wastewater addition experiments provided clear evidence of inner filter effects with the *in situ* (Manta) sensors, complicating their use in highly contaminated water. The benchtop fluorometer (Aqualog) corrects for inner filter effects using an algorithm based on the UV-visible absorbance spectrum. Submersible UV-visible absorbance sensors hold promise for correcting inner filter effects in real time.[36] Similar to ref 12, turbidity depressed TRP and CDOM of the *in situ* sensor by up to 80%, while the benchtop fluorometer (Aqualog) does not have turbidity interference since it uses a filtered sample. We calibrated the turbidity correction (k) value (eq 1) to the observed *E. coli* values (Figure 4), which may not be transferable among events or locations. The dummy variable of event date was a significant predictor of *E. coli* when included in the model with Manta TRP and Manta CDOM (Table 1), suggesting that the turbidity correction (k value), or the relationship between TRP and *E. coli*, varies by event. Future work is needed to determine the impacts of sediment type, including mineralogy, particle size and organic matter content, on the k value. Our results suggest that a turbidity correction is possible, but that the correction function and its parameters may vary over space and time.

TRP and CDOM values from the benchtop fluorometer (Aqualog) correlated more consistently with both pctWW in the laboratory experiments and with *E. coli* in the field samples than did the submersible *in situ* sensor (Manta). We conclude that the benchtop scanning fluorometer can estimate both percent wastewater and *E. coli*, and can be used as a benchmark for longer-term studies. The main limitations in estimating percent wastewater are, first, knowing the TRP of the untreated wastewater endmember at the time of sampling, since wastewater composition varies diurnally and seasonally. Ideally, measurements of TRP in streams would be accompanied by measurements of TRP in wastewater during the same sampling event. Second, other, nonwastewater sources of TRP and *E. coli*, including animal agriculture, may contribute to TRP readings, especially during storm events.

5.2. Implications for Monitoring Natural Waters. *In situ* fluorescence sensors are increasingly used for monitoring water in wastewater treatment plants, drinking water supplies and groundwater.[9,10,14,15,37] Similar to ref 21, we conclude that portable and *in situ* sensors may not yet be capable of monitoring water with high percentages of wastewater and have strong interference from turbidity and inner filter effects from organic matter. By contrast, the benchtop fluorometer outperformed the *in situ* sensors because the benchtop fluorometer included 1) sample filtration prior to measurement, which removes turbidity effects and 2) collection of multiple combinations of excitation and emission wavelengths, which allows for removing inner filter effects. Benchtop instruments hold promise for consistent long-term monitoring, but water samples must be collected, brought to the laboratory, and filtered prior to analysis. In river water, TRP proxies for percent wastewater show significant dilution but also additional source mobilization during storms; use of TRP as a sole surrogate for percent wastewater requires further documentation that other sources, especially runoff from animal agricultural operations, are not important contributors to TRP values. Alternatively, the wastewater discharge estimated with TRP can be interpreted as having a mix of human and nonhuman sources, both of which can impact human health. We recommend *in situ* TRP sensors for water with low (<40%) percent untreated wastewater, correction of turbidity during storm events, and benchtop (Aqualog) TRP measurements for waters with high (>40%) wastewater and to provide a baseline for comparison among events. *In situ* sensors that collect at several excitation−emission wavelength-pairs hold promise for real-time correction of inner filter effects,[36] and local calibration of turbidity correction factors due to particle size differences[38] could improve TRP estimations during storm events. Future turbidity corrections could be further improved by including data from *in situ* particle size analyzers.[39] The relationships between discharge, wastewater and bacteria developed here can provide the basis for loading estimates for studies of coastal contamination, but real-time *in situ* measurements require additional work for accurate correction of turbidity and inner filter effects in highly polluted waters.

■ ASSOCIATED CONTENT

Data Availability Statement

The data are available on HydroShare: Biggs, T., N. Mladenov, S. Garcia, Y. Yuan, D. Sousa, A. Grant, E. Piazza, T. Magdalena-Weary, C. Summerlin, D. Liden (2025). E. coli and fluorescence of the Tijuana River, 2022−2023, HydroShare, https://doi.org/10.4211/hs.8cdf887804df444fa85f37b4b5977a69.

Supporting Information

The Supporting Information is available free of charge at https://pubs.acs.org/doi/10.1021/acsestwater.4c01092.

Additional experimental details, calibration data, and additional results of laboratory turbidity experiments, comparison of TRP and CDOM from Aqualog and Manta sensors, sensitivity analysis of turbidity correction factors, regression values for nonlog transformed values, estimates of fecal coliform production from humans and animal agriculture, and maps of wastewater generation rates in Tijuana (PDF)

■ AUTHOR INFORMATION

Corresponding Author

Trent Biggs − *Department of Geography, San Diego State University, San Diego, California 92182, United States;* orcid.org/0000-0003-4978-1779; Email: tbiggs@sdsu.edu

Authors

Natalie Mladenov − *Department of Civil, Construction, and Environmental Engineering, San Diego State University, San Diego, California 92182, United States;* orcid.org/0000-0002-6984-2180

Stephany Garcia − *Department of Geography, San Diego State University, San Diego, California 92182, United States; Southwest Wetlands Interpretive Association, Imperial Beach, California 91932, United States*

Yongping Yuan − *United States Environmental Protection Agency-Office of Research and Development, Research Triangle Park, North Carolina 27711, United States*
Daniel Sousa − *Department of Geography, San Diego State University, San Diego, California 92182, United States*
Alexandra Grant − *Department of Civil, Construction, and Environmental Engineering, San Diego State University, San Diego, California 92182, United States*
Elise Piazza − *Department of Geography, San Diego State University, San Diego, California 92182, United States*
Trinity Magdalena-Weary − *Department of Civil, Construction, and Environmental Engineering, San Diego State University, San Diego, California 92182, United States*
Callie Summerlin − *Department of Geography, San Diego State University, San Diego, California 92182, United States*
Doug Liden − *United States Environmental Protection Agency-Region 9 Water Division, San Diego, California 92101, United States*

Complete contact information is available at: https://pubs.acs.org/10.1021/acsestwater.4c01092

Author Contributions

CRediT: **Trent Biggs** conceptualization, data curation, formal analysis, funding acquisition, methodology, project administration, supervision, writing - original draft; **Natalie Mladenov** conceptualization, formal analysis, investigation, methodology, supervision, writing - review & editing; **Stephany Garcia** data curation, investigation, methodology, supervision, writing - review & editing; **Yongping Yuan** conceptualization, funding acquisition, project administration, resources, supervision, writing - review & editing; **Daniel Sousa** conceptualization, funding acquisition, supervision, writing - review & editing; **Alexandra Grant** data curation, investigation, methodology, supervision, writing - review & editing; **Elise Piazza** data curation, investigation, supervision, writing - review & editing; **Trinity Magdalena-Weary** data curation, investigation, methodology, writing - review & editing; **Callie Summerlin** data curation, investigation, methodology; **Doug Liden** conceptualization, funding acquisition, methodology, project administration, resources, supervision, writing - review & editing.

Funding

This work was funded by the Environmental Protection Agency (PR-ORD-21-01804), J.W. Sefton Foundation, the National Aeronautics and Space Administration (80NSSC22K0907 and 80NSSC23K1460) and full fellowship support to Stephany Garcia from the National Oceanic and Atmospheric Administration − Cooperative Science Center for Earth System Sciences and Remote Sensing Technologies under the Cooperative Agreement Grant NA22SEC4810016.

Notes

The authors declare no competing financial interest.

■ ACKNOWLEDGMENTS

Morgan Rogers and Samuel Katzenstein from the International Boundary and Water Commission provided permission and assistance with site access and installation. Pablo Bryant (SDSU Field Stations) designed and led the Manta installation and maintenance. Student assistants included Keyshawn Ford, Elisa Rivera, Isaiah Hand, and Elena Aguilar. Two anonymous reviewers provided helpful comments that improved the paper. This manuscript has been reviewed and approved for publication by the US EPA, but the views expressed in this manuscript are those of the authors and do not necessarily represent the views or policies of the EPA, NOAA, or NASA.

■ REFERENCES

(1) Reifel, K. M.; Johnson, S. C.; DiGiacomo, P. M.; Mengel, M. J.; Nezlin, N. P.; Warrick, J. A.; Jones, B. H. Impacts of Stormwater Runoff in the Southern California Bight: Relationships among Plume Constituents. *Cont. Shelf Res.* **2009**, *29* (15), 1821−1835.
(2) Stein, E. D.; Ackerman, D. Dry Weather Water Quality Loadings in Arid, Urban Watersheds of the Los Angeles Basin, California, USA1. *JAWRA* **2007**, *43* (2), 398−413.
(3) Feddersen, F.; Boehm, A. B.; Giddings, S. N.; Wu, X.; Liden, D. Modeling Untreated Wastewater Evolution and Swimmer Illness for Four Wastewater Infrastructure Scenarios in the San Diego-Tijuana (US/MX) Border Region. *GeoHealth* **2021**, *5* (11), No. e2021GH000490.
(4) Baker, A. Fluorescence Properties of Some Farm Wastes: Implications for Water Quality Monitoring. *Water Res.* **2002**, *36* (1), 189−195.
(5) Baker, A.; Cumberland, S. A.; Bradley, C.; Buckley, C.; Bridgeman, J. To What Extent Can Portable Fluorescence Spectroscopy Be Used in the Real-Time Assessment of Microbial Water Quality? *Sci. Total Environ.* **2015**, *532*, 14−19.
(6) Cumberland, S.; Bridgeman, J.; Baker, A.; Sterling, M.; Ward, D. Fluorescence Spectroscopy as a Tool for Determining Microbial Quality in Potable Water Applications. *Environ. Technol.* **2012**, *33* (6), 687−693.
(7) Carstea, E. M.; Bridgeman, J.; Baker, A.; Reynolds, D. M. Fluorescence Spectroscopy for Wastewater Monitoring: A Review. *Water Res.* **2016**, *95*, 205−219.
(8) Mendoza, L. M.; Mladenov, N.; Kinoshita, A. M.; Pinongcos, F.; Verbyla, M. E.; Gersberg, R. Fluorescence-Based Monitoring of Anthropogenic Pollutant Inputs to an Urban Stream in Southern California, USA. *Sci. Total Environ.* **2020**, *718*, 137206.
(9) Sorensen, J. P. R.; Carr, A. F.; Nayebare, J.; Diongue, D. M. L.; Pouye, A.; Roffo, R.; Gwengweya, G.; Ward, J. S. T.; Kanoti, J.; Okotto-Okotto, J.; Van Der Marel, L.; Ciric, L.; Faye, S. C.; Gaye, C. B.; Goodall, T.; Kulabako, R.; Lapworth, D. J.; MacDonald, A. M.; Monjerezi, M.; Olago, D.; Owor, M.; Read, D. S.; Taylor, R. G. Tryptophan-like and Humic-like Fluorophores Are Extracellular in Groundwater: Implications as Real-Time Faecal Indicators. *Sci. Rep.* **2020**, *10* (1), 15379.
(10) Sorensen, J. P. R.; Lapworth, D. J.; Marchant, B. P.; Nkhuwa, D. C. W.; Pedley, S.; Stuart, M. E.; Bell, R. A.; Chirwa, M.; Kabika, J.; Liemisa, M.; Chibesa, M. In-Situ Tryptophan-like Fluorescence: A Real-Time Indicator of Faecal Contamination in Drinking Water Supplies. *Water Res.* **2015**, *81*, 38−46.
(11) Goldman, J. H.; Rounds, S. A.; Needoba, J. A. Applications of Fluorescence Spectroscopy for Predicting Percent Wastewater in an Urban Stream. *Environ. Sci. Technol.* **2012**, *46* (8), 4374−4381.
(12) Khamis, K.; Sorensen, J. P. R.; Bradley, C.; Hannah, D. M.; Lapworth, D. J.; Stevens, R. In Situ Tryptophan-like Fluorometers: Assessing Turbidity and Temperature Effects for Freshwater Applications. *Environ. Sci.: Processes Impacts* **2015**, *17* (4), 740−752.
(13) Nowicki, S.; Lapworth, D. J.; Ward, J. S. T.; Thomson, P.; Charles, K. Tryptophan-like Fluorescence as a Measure of Microbial Contamination Risk in Groundwater. *Sci. Total Environ.* **2019**, *646*, 782−791.
(14) Sorensen, J. P. R.; Nayebare, J.; Carr, A. F.; Lyness, R.; Campos, L. C.; Ciric, L.; Goodall, T.; Kulabako, R.; Curran, C. M. R.; MacDonald, A. M.; Owor, M.; Read, D. S.; Taylor, R. G. In-Situ Fluorescence Spectroscopy Is a More Rapid and Resilient Indicator of Faecal Contamination Risk in Drinking Water than Faecal Indicator Organisms. *Water Res.* **2021**, *206*, 117734.
(15) Ward, J. S. T.; Lapworth, D. J.; Read, D. S.; Pedley, S.; Banda, S. T.; Monjerezi, M.; Gwengweya, G.; MacDonald, A. M. Tryptophan-like Fluorescence as a High-Level Screening Tool for

Detecting Microbial Contamination in Drinking Water. *Sci. Total Environ.* **2021**, *750*, 141284.
(16) Wasswa, J.; Mladenov, N. Improved Temperature Compensation for In Situ Humic-Like and Tryptophan-Like Fluorescence Acquisition in Diverse Water Types. *Environ. Eng. Sci.* **2018**, *35* (9), 971−977.
(17) Lakowicz, J. *Principles of Fluorescence Spectroscopy*; Kluwer Academic Publishers: Dordrecht, The Netherlands, 1999.
(18) Stedmon, C. A.; Markager, S.; Bro, R. Tracing Dissolved Organic Matter in Aquatic Environments Using a New Approach to Fluorescence Spectroscopy. *Mar. Chem.* **2003**, *82* (3−4), 239−254.
(19) Goffin, A.; Vasquez-Vergara, L. A.; Guérin-Rechdaoui, S.; Rocher, V.; Varrault, G. Temperature, Turbidity, and the Inner Filter Effect Correction Methodology for Analyzing Fluorescent Dissolved Organic Matter in Urban Sewage. *Environ. Sci. Pollut. Res.* **2020**, *27* (28), 35712−35723.
(20) Hansen, A. M.; Fleck, J.; Kraus, T. E. C.; Downing, B. D.; von Dessonneck, T.; Bergamaschi, B. A. *Procedures for Using the Horiba Scientific Aqualog® Fluorometer to Measure Absorbance and Fluorescence from Dissolved Organic Matter*; Open-File Report, Report 2018−1096: Reston, VA, 2018. .
(21) Downing, B. D.; Pellerin, B. A.; Bergamaschi, B. A.; Saraceno, J. F.; Kraus, T. E. C. Seeing the Light: The Effects of Particles, Dissolved Materials, and Temperature on in Situ Measurements of DOM Fluorescence in Rivers and Streams. *Limnol. Oceanogr.: Methods* **2012**, *10* (10), 767−775.
(22) Biggs, T.; Zeigler, A.; Taniguchi-Quan, K. T. Runoff and Sediment Loads in the Tijuana River: Dam Effects, Extreme Events, and Change during Urbanization. *J. Hydrol.* **2022**, *42*, 101162.
(23) Instituto Nacional de Estadística y Geografía *Principales Resultados Del Censo de Población y Vivienda 2020*: Baja California, 2023. https://www.inegi.org.mx/contenidos/productos/prod_serv/contenidos/espanol/bvinegi/productos/nueva_estruc/702825198084.pdf.
(24) Instituto Nacional de Estadística y Geografía *Censo Agropecuario*; INEGI: Baja California, Aguascalientes, Mexico, 2022.
(25) Aguado, E. Temperature. In *Tijuana River Watershed Atlas/Atlas de la Cuenca del río Tijuana*; Wright, R.; Vela, R.; Ganster, P., Eds.; San Diego State University Press: San Diego, CA, USA, 2005.
(26) Deméré, T. A. Geology: Generalized Rock Types and Faults. In *Tijuana River Watershed Atlas/Atlas de la Cuenca del río Tijuana*; Wright, R.; Vela, R.; Ganster, P., Eds.; San Diego State University Press: San Diego, CA, USA.
(27) HDR *Tijuana River Valley Needs and Opportunities Assessment*; HDR: San Diego, CA, USA, 2020.
(28) Mladenov, N.; Biggs, T.; Ford, K.; Garcia, S.; Yuan, Y.; Grant, A.; Piazza, E.; Rivera, E.; Pinongcos, F.; Keely, S. P.; Summerlin, C.; Crooks, J. A.; Liden, D. Evaluation of Real-Time Fluorescence Sensors and Benchtop Fluorescence for Tracking and Predicting Sewage Contamination in the Tijuana River Estuary at the US-Mexico Border. *Sci. Total Environ.* **2024**, *950*, 175137.
(29) Maione, C.; Vito, D.; Fernandez, G. Monitoring the Effects of Transboundary Water Pollution in Imperial Beach, California. *Med. Sci. Forum.* **2024**, *25*, 14.
(30) Eureka Water Probes *Manta and Trimeter Multiprobe Manual*; Eureka Water Probes: Austin, Texas, USA, 2018.
(31) U.S. Environmental Protection Agency *Method 1603: Escherichia Coli (E. Coli) in Water by Membrane Filtration Using Modified Membrane-Thermotolerant Escherichia Coli Agar*; Modified mTEC. EPA-821-R-04−025; Office of Water: Washington, D.C., 2005.
(32) Hoaglin, D. C.; Iglewicz, B.; Tukey, J. W. Performance of Some Resistant Rules for Outlier Labeling. *J. Am. Stat. Assoc.* **1986**, *81* (396), 991−999.
(33) Atinkpahoun, C. N. H.; Le, N. D.; Pontvianne, S.; Poirot, H.; Leclerc, J.-P.; Pons, M.-N.; Soclo, H. H. Population Mobility and Urban Wastewater Dynamics. *Sci. Total Environ.* **2018**, *622−623*, 1431−1437.
(34) Lu, M.; Li, Z.-H.; Jiang, Y. Effluent Temporal Collective Behaviors of a Wastewater Treatment Plant Community. *Sci. Total Environ.* **2021**, *787*, 147694.
(35) Lee, H.; Lau, S.-L.; Kayhanian, M.; Stenstrom, M. K. Seasonal First Flush Phenomenon of Urban Stormwater Discharges. *Water Res.* **2004**, *38* (19), 4153−4163.
(36) Goffin, A.; Varrault, G.; Musabimana, N.; Raoult, A.; Yilmaz, M.; Guérin-Rechdaoui, S.; Rocher, V. Improving Monitoring of Dissolved Organic Matter from the Wastewater Treatment Plant to the Receiving Environment: A New High-Frequency in Situ Fluorescence Sensor Capable of Analyzing 29 Pairs of Ex/Em Wavelengths. *Spectrochim. Acta, Part A* **2025**, *325*, 125153.
(37) Mladenov, N.; Bigelow, A.; Pietruschka, B.; Palomo, M.; Buckley, C. Using Submersible Fluorescence Sensors to Track the Removal of Organic Matter in Decentralized Wastewater Treatment Systems (DEWATS) in Real Time. *Water Sci. Technol.* **2018**, *77* (3), 819−828.
(38) Saraceno, J. F.; Shanley, J. B.; Downing, B. D.; Pellerin, B. A. Clearing the Waters: Evaluating the Need for Site-specific Field Fluorescence Corrections Based on Turbidity Measurements. *Limnol. Oceanogr.: Methods* **2017**, *15* (4), 408−416.
(39) Brown, J. S.; Ackerman, D.; Stein, E. D. Continuous In Situ Characterization of Particulate Sizes in Urban Stormwater: Method Testing and Refinement. *J. Environ. Eng.* **2012**, *138* (6), 673−679.

https://doi.org/10.1021/acsestwater.4c01092
ACS EST Water 2025, 5, 2212−2222